Philosophical Magazine A
Publication details, including instructions for authors and subscription information:
http://www.tandfonline.com/loi/tpha20

Structures and energies of compression twin boundaries in hcp Ti and Zr

J. R. Morris [a] , Y. Y. Ye [a] , K. M. Ho [a] , C. T. Chan [a] & M. H. Yoo [b]

[a] Ames Laboratory—US Department of Energy, Department of Physics and Astronomy , Iowa State University , Ames, IA, 50011, USA

[b] Metals and Ceramics Division, Oak Ridge National Laboratory , Oak Ridge, TN, 37831-6115, USA

Published online: 27 Sep 2006.

To cite this article: J. R. Morris , Y. Y. Ye , K. M. Ho , C. T. Chan & M. H. Yoo (1995) Structures and energies of compression twin boundaries in hcp Ti and Zr, Philosophical Magazine A, 72:3, 751-763, DOI: 10.1080/01418619508243798

To link to this article: http://dx.doi.org/10.1080/01418619508243798

PHILOSOPHICAL MAGAZINE A, 1995, VOL. 72, NO. 3, 751–763

Structures and energies of compression twin boundaries in *hcp* Ti and Zr

By J. R. MORRIS, Y. Y. YE, K. M. HO, C. T. CHAN

Ames Laboratory—US Department of Energy,
Department of Physics and Astronomy,
Iowa State University, Ames, IA 50011, USA

and M. H. YOO

Metals and Ceramics Division, Oak Ridge National Laboratory Oak Ridge,
TN 37831-6115, USA

[*Received 19 October 1994 and accepted 8 February 1995*]

ABSTRACT

Using a combination of first-principles and embedded-atom techniques, we have calculated the structure and energy of compression twin boundaries in hcp Zr and Ti, the most ductile of the hcp elements. These calculations are important tests of classical nucleation theory, which predicts that the energy of these structures controls the nucleation rate. Our results contradict this: the $\{11\bar{2}2\}$ twin boundary, which is prevalent at low temperatures, is significantly higher in energy than the competing $\{10\bar{1}1\}$ twin which is only formed at higher temperatures.

§ 1. INTRODUCTION

Most textbook discussions on the strength and ductility of materials concentrate on slip processes and the associated dislocation movement. However, in materials such as hcp metals which have a limited number of slip modes, these properties are often controlled by twinning. This has attracted more attention in recent years due to the fact that in many materials of interest, such as the Ti-aluminides, twinning (or lack thereof) strongly influences the strength and ductility (Yoo 1981, Yoo, Fu and Lee 1991).

Currently, there is little understanding of what factors determine whether or not a material will easily form twins. In particular, the formation of twin boundaries is poorly understood. The hcp elemental metals are an ideal starting point for trying to understand twinning phenomena, because of their relative simplicity, and because there is a broad range of ductilities.

The most ductile hcp metals are Ti and Zr, which have four different twinning modes (Yoo 1981). In this paper, we will concentrate on the 'compression twins' which are formed under conditions of c-axis compression. For single-crystal Ti and Zr at relatively low temperatures ($\leqslant 600$ K for Ti and $\leqslant 800$ K for Zr), the formation of $\{11\bar{2}2\}$ twins by c-axis compression accounts for nearly all of the plastic deformation (Paton and Backofen 1970, Akhtar 1973). The twin formation is accompanied by a load drop, whose magnitude increases with temperature. This indicates a nucleation barrier that increases with temperature. The strength of the materials also increases with temperature.

As the materials are heated above these temperatures, there is a rapid change in behaviour, occurring over a range of approximately 50 K. At these higher temperatures,

Ti and Zr primarily deform by **c** + **a** slip along the $\langle 11\bar{2}2\rangle$ direction, along with some $\{10\bar{1}1\}$ twinning. The amount of twinning decreases as the temperature increases. There are no stress drops associated with the plastic deformation, and the yield strength decreases with increasing temperature. Slip occurs in the same direction as the low-temperature twinning shear direction, viz. along the $[12\bar{2}\bar{3}]$ direction. This suggests that this dramatic change in behaviour as a function of temperature is a crossover between $\{11\bar{2}2\}$ twinning and $\{11\bar{2}2\}$ slip (Rosenbaum 1964).

Classical nucleation theory predicts that in order for the $\{11\bar{2}2\}$ twin to be favoured at low temperatures, the ratio of the twin boundary energies should satisfy $\Gamma(10\bar{1}1)/\Gamma(11\bar{2}2) > 0{\cdot}9$ (Yoo and Lee 1991). In order to test this, and to examine growth processes, many workers have used empirical atomistic models to examine the structures and energies of twin boundaries, as well as the twinning dislocations associated with twin growth by boundary movement (Serra and Bacon 1986, 1991, 1993, Serra, Pond and Bacon 1991, Yoo and Lee 1991, Bacon and Serra 1992). The difficulty of such models is that they are not fully comparable to real materials. Different models produce very similar structures for the twin boundaries and dislocations, but twin boundary energies vary greatly. These workers have not attempted to support their calculations with less empirical techniques, so it is difficult to draw conclusions about real materials from the predicted energies. In particular, there has not been any significant work that explains why Be, which is quite brittle and has only one active twinning mode, is so different from Ti and Zr.

With this in mind, we have used first-principle calculations, along with an empirical potential, to calculate twin boundary structures in Ti and Zr. The first-principles calculations are based upon a fully quantum-mechanical calculation of the energy of the structure. The advantage of first-principles calculations is that they do not require any empirical information, are significantly more accurate than empirical modelling, and are fully transferable.

Using these techniques, this paper conclusively demonstrates that for Ti and Zr, the $\{10\bar{1}1\}$ twin boundary energy is significantly lower than the $\{11\bar{2}2\}$ twin energy, which would imply (from classical nucleation theory) that it should be favoured (Morris, Ye, Ho, Chan and Yoo 1994). We believe that this discrepancy is due to the fact that classical nucleation theory assumes that the surface energy density of the nucleus boundary is constant, independent of the orientation. In fact, it will depend not only upon the orientation, but may also include other types of defect (such as twinning dislocations) which will affect the boundary energy in non-trivial ways. Further, the classical theory does not incorporate atomistic motions ('shuffling'), which is important when the unit cell has a basis, as in the hcp metals (Yoo *et al.* 1991).

This paper is an extension of the work of Morris *et al.* (1994), where we presented calculations for the structure and energy of Zr compression twin boundaries. In that paper, we used an embedded atom method (EAM) to generate starting structures which were then further relaxed using first-principles techniques. Here, we begin by detailing the Zr EAM model used here and in Morris *et al.* (1994), and review the results from this model. We then present our results for the twin boundary energies and structures of Ti and Zr found from first-principles calculations.

§ 2. EAM MODEL OF Zr

Before performing the first-principles calculations, we used an empirical model of Zr to explore the possible twin structures. This model has been used previously to explore the pretransitional dynamics of the bcc → hcp transition (Zhang, Wang, Ho,

Turner and Ye 1995). In this section, we give details of this model, along with some of the properties of the bcc and hcp structure given by this model.

In choosing an empirical form, we decided upon an EAM model (Daw and Baskes 1983, 1984, Daw, Foiles, and Baskes 1993) due to its relative simplicity, and due to the fact that it incorporates many-body forces. It is important to go beyond pair potentials, due to their well-known unphysical characteristics. For example, using pair potentials to model cubic systems always satisfies the 'Cauchy relation', namely $C_{12} = C_{44}$. Real materials typically do not satisfy this condition. Further, for pair potentials, the energy of an atom depends directly upon the number of neighbouring atoms—a structure with more near neighbours will usually be significantly lower in energy than a more open structure. For many-body potentials and in real materials, the bonding will tend to saturate, so that adding more neighbours is not as strongly preferred.

The EAM models (and equivalent forms, such as the Finnis–Sinclair potentials (Finnis and Sinclair 1984)) are the simplest many-body potentials, as they are functionals of pair interactions. The EAM energy is (Daw and Baskes 1983, 1984)

$$U = \sum_i F(\rho_i) + \sum_{j>i} \frac{Z^2(r_{ij})}{r_{ij}}, \tag{1}$$

where the local charge density is

$$\rho_i = \sum_{j \neq i} f(r_{ij}). \tag{2}$$

In eqn. (1), $F(\rho)$ is the energy associated with embedding an ion into an area with charge density ρ. This charge density is calculated as a superposition of atomic densities

Table 1. Spline tables for EAM model of zirconium. Note that the values for $F(\rho)$ are in eV.

$\rho/\bar{\rho}, \bar{\rho} = 0{\cdot}0332$	$F(\rho)$	r/r_0, $r_0 = 3{\cdot}23$ Å	$Z(r)$
0·00	0·00	0·00	40·0
0·50	−7·1227941	0·50	10·0908955
1·00	−11·137418	0·95	0·50885
2·00	−7·5205386	1·35	0·0858802
2·25	0·00	2·05	0·00

Table 2. Comparison of EAM values with experiment and first-principles calculations.

	EAM	First principles	Experiment	Reference
hcp phase:				
E_{coh} (eV)	6·25	7·26	6·25	Brewer 1975
a_0 (Å)	3·22	3·18	3·23	Goldak *et al.* 1966
c/a ratio	1·62	1·61	1·592	Goldak *et al.* 1966
B (Mbar)	1·5	1·1	0·97	Fisher and Renken 1964
C_{33} (Mbar)	1·8	0·00	1·725	Fisher and Renken 1964
bcc phase:				
E_{coh} (eV)	6·23	7·19	—	
a_0 (Å)	3·60	3·52	3·57	Heiming *et al.* 1988
B (Mbar	0·93	1·04	0·97	Heiming *et al.* 1988

specified by $f(r)$. (For a thorough discussion of the failures of pair potentials and the advantages and limitations of EAM potentials, see Daw *et al.* (1993).)

To model Zr, we developed spline tables for the functions $F(\rho)$ and $Z(r)$ in eqn. (1), following the work of Daw (Daw and Baskes 1983). The spline tables are given in table 1. The atomic charge densities $f(r)$ used in eqn. (2) were calculated using spline tables from the calculations in Clementi and Roetti (1974) and Sinclair and Fletcher (1972).

The model values for a number of physical properties, including the lattice constant

Fig. 1

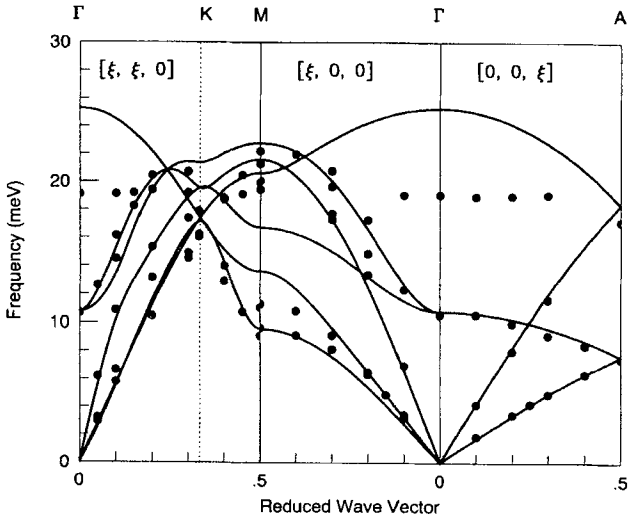

Phonons for the EAM model of hcp Zr (solid lines) compared with the experimental results of Stassis *et al.* (1978) (●).

Fig. 2

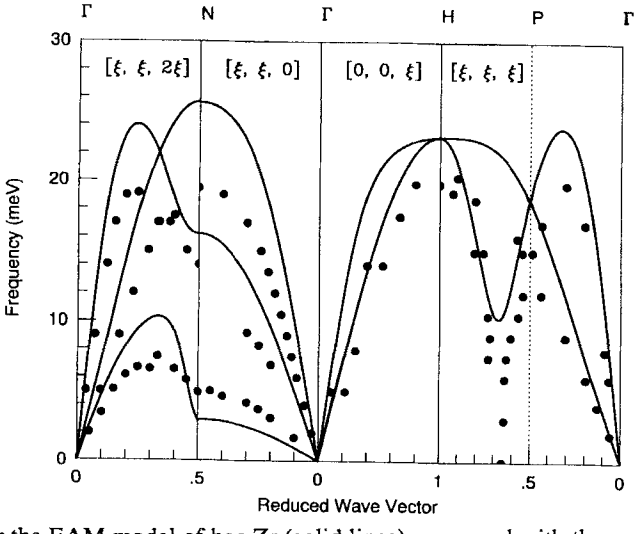

Phonons for the EAM model of bcc Zr (solid lines) compared with the experimental results of Heiming *et al.* (1988) (●).

and the *c/a* ratio for the hcp phase, are compared with first-principles calculations and with experimental results in table 2. We have included some of the values for the bcc phase, which, for this model, is metastable. The physical values are in generally good agreement with the first principles and the experimental values. We have also calculated the phonons for the hcp and bcc structures using this model, as this is a more stringent test than the elastic constants. These are shown in figs. 1 and 2. Our results are in good agreement with the experimental results (Stassis, Zaretsky, Arch, McMasters and Harmon 1978, Heiming *et al.* 1988), especially for the hcp phase.

We note that although the EAM provides for many-body forces, it neglects bond-bending forces that can be important in determining structures and energetics. This can result in incorrect predictions of structures (Campbell, Foiles, Gumbsch, Rühle and King 1993). However, we feel that our results are supported by the fact that previous empirical models for twin boundaries in hcp twins have consistently produced structures quite similar to ours. More importantly, our results from the first-principles calculations have given energies qualitatively similar to those of the model. We will discuss this in more details in § 5.

§ 3. Determination of twin structures from the EAM model

With the above model, we may construct possible twin boundary structures. One difficulty in calculating twin boundary energies is that there is a variety of possible structures that should be considered. The twin boundary may be a mirror plane through a plane of atoms, between planes of atoms, or may not be a mirror plane at all. Exploring these possibilities using first-principles calculations would certainly be desirable, but is not feasible due to the computational requirements.

With this in mind, we have generated starting geometries for the first-principles calculations by creating various twin structures which were then relaxed using the above EAM model. We tried numerous possibilities, including: (1) the unrelaxed mirror twin; (2) the unrelaxed mirror twin with the atoms on the mirror plane removed; (3) the unrelaxed twin with the atoms on one side of the twin shifted along the shear direction; and (4) the unrelaxed twin, with the atoms on the twin plane removed, and with half the atoms shifted as in (3). The various starting points were sufficient to explore the possible symmetries associated with these particular twin boundaries (Pond, Bacon, Serra and Sutton 1991). All structures were relaxed, annealed at $T = 1000$ K, and then relaxed again. In all cases, the same resultant structure was obtained, independent of the starting configuration.

For the $\{10\bar{1}1\}$ twin, there are some particular difficulties, due to the fact that there are pairs of closely spaced planes of atoms parallel to the twin boundary. This can be seen in fig. 3, which shows the relaxed $\{10\bar{1}1\}$ twin structure. The final structure is formed by collapsing a pair of these planes together, forming a single plane of atoms along the twin boundary. Previous studies (Serra and Bacon 1991, 1993, Serra *et al.* 1991, Yoo and Lee 1991, Bacon and Serra 1992) have assumed this structure; for our work, we found that this occurred naturally in the relaxation process. We specifically searched for a stable glide twin, as this has been suggested by recent experiments (Kasukabe, Yamada, Lin, Ju and Bursill 1993), but were unable to do so. The low energy of the $\{10\bar{1}1\}$ twin boundary (see table 3) strongly suggests that this is the lowest energy twin boundary structure.

The final relaxed structures for both twins, shown in figs. 3 and 4, are very similar to structures obtained from other models of hcp metals (Serra and Bacon 1991, 1993, Serra *et al.* 1991, Yoo and Lee 1991, Bacon and Serra 1992). The energies of the twin

Fig. 3

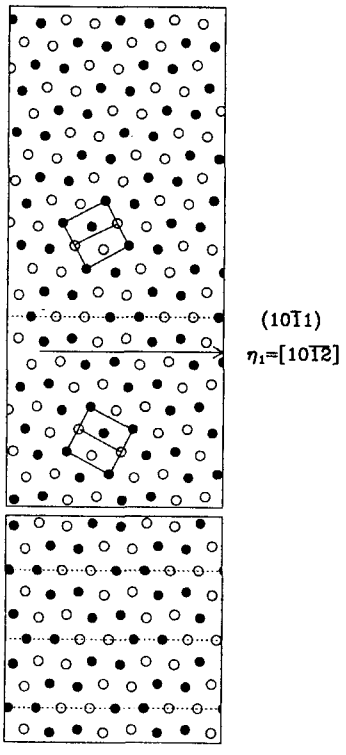

Structure of the {10$\bar{1}$1} twin boundary calculated using the EAM model of Zr. Different symbols indicate atoms at different depths. The shear direction necessary to form the upper bicrystal from the lower part is $\eta_1 = \frac{1}{3}[10\bar{1}\bar{2}]$.

boundaries are shown in table 3. In both cases, the twin plane is indeed a mirror plane. The primary relaxation from an unrelaxed mirror twin is expansion perpendicular to the twin plane. This relaxation is shown in fig. 5, with the component of relaxation along the direction η_1. There is no significant relaxation perpendicular to these two directions. Note that for distances greater than about 5 Å, the atomic relaxation is simply a uniform displacement from the twin boundary. This should cause a coupling to stress components *normal* to the twin boundary, which in principle should affect the nucleation rate. However, we expect that this effect will be small.

We may estimate the magnitude of the effect of normal stress in the following manner. The 'core' of the {11$\bar{2}$2} twin boundary (measured by the total expansion perpendicular to the twin boundary) is approximately 0·2 Å, as can be seen in fig. 5. For Zr, the stress at which the first load drops due to {11$\bar{2}$2} twinning is approximately 2×10^7 N m^{-2}, at low temperatures (Akhtar 1973). Taking this as a rough estimate of the external normal stress, the energy to expand the system by 0·2 Å is approximately 0·4 mJ m^{-2}. For the {10$\bar{1}$1} twin, the expansion is approximately twice as much, so we would expect a somewhat larger number. However, comparing these additional energies to the calculated twin boundary energies (see table 2) reveals that these differences are insignificant. This is in accord with recent work that examined the role of normal stress (Lebensohn and Tomé 1993). The actual effect will probably be smaller than this estimate, as only a fraction of the applied stress will be normal to the twin plane.

Fig. 4

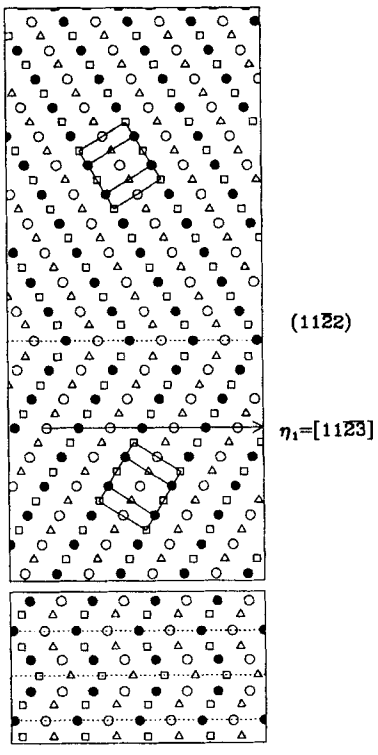

Structure of the {11$\bar{2}$2} twin boundary calculated using the EAM model of Zr. Different symbols indicate atoms at different depths. The shear direction necessary to form the upper bicrystal from the lower part is $\eta_1 = \frac{1}{3}[11\bar{2}\bar{3}]$.

§ 4. Structure determination using first-principles calculations

In order to further verify the structures, and to calculate reliable twin boundary energies, we feel that it is necessary to go beyond empirical potentials, such as our EAM model. These models are developed by fitting to the equilibrium structure, and may not give accurate results for the energy or structure of defects that have significantly different structures from the bulk phase. First-principles calculations do not rely upon empirical fitting to known properties, and they accurately predict the energetics of very different structures of the same material. For Ti and Zr in particular, first-principles calculations have been able to establish the relative energetics of the hcp, bcc and ω-phases, without any fitting. In addition, by using the 'frozen phonon' approach, first-principles calculations have been able to predict the phonon frequency and the energy barrier associated with the bcc → ω transition (Ho, Fu and Harmon 1984, Chen, Fu, Ho and Harmon 1985).

However, such an approach is computationally more difficult, and we are restricted to relatively small, periodic lattices. The calculation of the energy and the forces on the ions are quite time-consuming, so we must start off with a configuration that is fairly close to fully relaxed. This is the advantage of starting with the EAM calculation: if the EAM predictions for the structures are reasonably good, then little further relaxation should occur when using the more accurate technique. We have found that the EAM results for the energetics of the structures are reasonable, in comparison with other

Table 3. Twin boundary energies for Ti and Zr from first-principles calculations, from EAM model of Zr presented in this work, and from other empirical models from other authors.

Model	Γ_1, $\{10\bar{1}1\}$ k_BT_m/a^2	Γ_2, $\{11\bar{2}2\}$ k_BT_m/a^2	Ratio Γ_1/Γ_2
First-principles results			
Ti	0·35 ± 0·11	1·59 ± 0·07	0·22
Zr	0·29 ± 0·11	1·12 ± 0·06	0·26
EAM results			
Zr EAM (single twin)	0·57	0·97	0·57
Zr EAM (twin array)	0·53	0·91	0·58
Other calculations for hcp metals			
Zr FS (Serra and Bacon 1993)	0·80	0·87	0·92
Ti FS (Bacon and Serra 1992)	0·60	0·68	0·88
Mg FS (Serra and Bacon 1991)	1·15	1·17	0·98
na56 (Serra *et al.* 1991)	0·64	0·92	0·70
lj56 (Yoo and Lee 1991)	2·49	0·87	2·9

Fig. 5

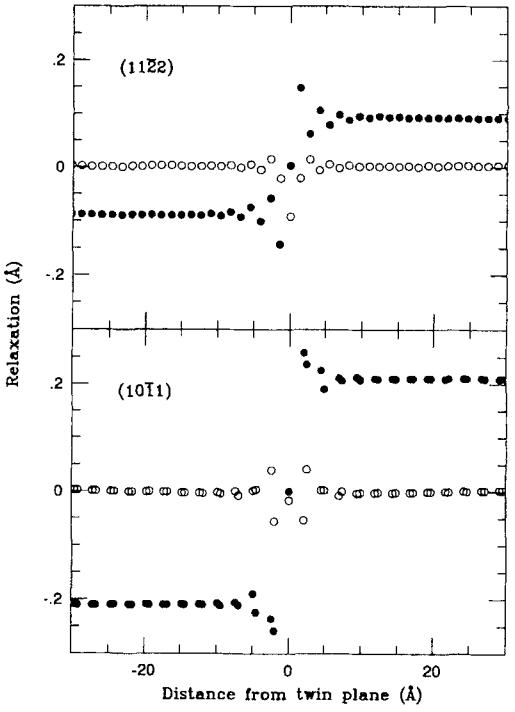

Relaxation normal to the twin boundary (●) and along the shear direction η_1 (○), relative to the unrelaxed mirror twin, for the $\{10\bar{1}1\}$ and the $\{11\bar{2}2\}$ twins. At distances greater than about 5 Å, the normal component of relaxation is essentially a uniform displacement away from the twin boundary.

calculations and with our final first-principles calculations, giving us confidence in our results. Furthermore, most empirical models have given similar structures to our EAM results, so we believe that the actual structures should be similar.

4.1. *Details of first-principles calculations*

We have used a self-consistent pseudopotential method, in which the local density approximation (LDA) (Jones and Gunnarsson 1991) for the total energy of a material may be written as (Ihm, Zunger and Cohen 1979)

$$E_T = \sum_i n_i \langle \psi_i | -\nabla^2 | \psi_i \rangle + \frac{1}{2} \int\int \frac{2\rho(\mathbf{r})\rho(\mathbf{r}')}{|\mathbf{r}-\mathbf{r}'|} \, d\mathbf{r}\, d\mathbf{r}' + \int \varepsilon_{xc}(\rho(\mathbf{r}))\, d\mathbf{r}$$
$$+ \sum_{\mathbf{R},\tau} \left[\int \rho(\mathbf{r}) V_{ps}^{L}(\mathbf{r}-\mathbf{R}-\tau)\, d\mathbf{r} + \sum_{i,l} n_i \langle \psi_i | V_{ps,l}^{NL}(\mathbf{r}-\mathbf{R}-\tau) \hat{P}_l | \psi_i \rangle \right]$$
$$+ \frac{1}{2} {\sum_{\mathbf{R},\mathbf{R}',\tau,\tau'}}' \frac{2Z_V^2}{|\mathbf{R}+\tau-\mathbf{R}'-\tau'|}, \tag{3}$$

where the prime in the summation means that the $|\mathbf{R}+\tau-\mathbf{R}'-\tau'|=0$ term is excluded; $\mathbf{R}$ denotes the lattice vector; τ denotes the basis vector; Z_V is the effective ionic charge; and ε_{xc} is the local exchange-correlation potential $\varepsilon_{xc}(\rho)$. We have used the Hedin–Lundquist form for the exchange-correlation potential (Hedin and Lundquist 1971). In eqn. (3), we have used atomic units, with $\hbar = 1$, $m_e = \frac{1}{2}$, and $e^2 = 2$ so that the units of energy are Rydbergs.

In eqn. (3), we have used a norm-conserving pseudopotential to describe the electron–ion interaction (Hamann, Schlüter and Chiang 1979, Kerker 1980). V_{ps}^{L} is the local part of the pseudopotential, acting equally on all of the angular momentum components of the wavefunction. The non-local part is defined as

$$V_{ps,l}^{NL}(\mathbf{r}) = V_{ps,l}(\mathbf{r}) - V_{ps}^{L}(\mathbf{r}), \tag{4}$$

where $V_{ps,l}$ and $\hat{P}_l$ are the core pseudopotential and the projection operator for angular momentum l, respectively. Thus, the long-range part (singular part) of the pseudopotential has been isolated to the local part, making $V_{ps,l}^{NL}$ short range.

In most band-theoretical methods, the electronic wavefunction is expanded in a set of basis functions and the solutions to the Schrödinger equation are obtained by variational procedures. For Ti and Zr, the localized character of the *d*-electrons makes the expansion for the wavefunctions in plane waves uneconomical. In order to treat a system with atomic-like character as well as extended character, an energy-independent basis set containing both plane waves (with a 15 Rydberg cut-off) and Bloch sums of localized orbitals are used to represent the electronic wavefunctions (Louie, Ho and Cohen 1979):

$$\psi_{n\mathbf{k}}(\mathbf{r}) = \frac{1}{\sqrt{\Omega}} \sum_{\mathbf{G}} \alpha_n(\mathbf{k}+\mathbf{G}) \exp[i(\mathbf{k}+\mathbf{G})\cdot\mathbf{r}] + \sum_{jm} \beta_{jm}(n,\mathbf{k}) \phi_{jm}(\mathbf{k},\mathbf{r}), \tag{5}$$

with

$$\phi_{jm}(\mathbf{k}, br) = \frac{1}{\sqrt{N}} \sum_{\mathbf{R}} \exp[i\mathbf{k}\cdot(\mathbf{R}+\tau_j)] f_{jm}(\mathbf{r}-\mathbf{R}-\tau_j). \tag{6}$$

In these equations, Ω is the crystal volume, N is the number of atoms and m is the label for the orbital on the jth atom. We have used $\mathbf{G}$ to denote reciprocal lattice vectors,

and **k** for wave-vectors within the first Brillouin zone. For the local *d*-orbital, we have used a numerical basis of the form

$$\begin{aligned} f'(r) &= Bf(r)[1 - \exp[-\alpha(r_c - r)^2]], \quad r \leqslant r_c, \\ &= 0, \qquad\qquad\qquad\qquad\quad r > r_c, \end{aligned} \tag{7}$$

where $f(r)$ is a radial function closely related to the radial distribution of the atomic *d*-wavefunction, B is a normalization constant, and α is determined variationally (Takeuchi, Chan and Ho 1989, Elsässer *et al.* 1990).

This mixed basis leads to the following matrix eigenvalue problem:

$$(\mathbf{H} - E\mathbf{S})\mathbf{\Lambda} = 0, \tag{8}$$

where **H** is the Hamiltonian matrix, E is the eigenvalue, **S** is the overlap matrix and $\mathbf{\Lambda}$ is a column vector with elements $\lambda_1, \ldots, \lambda_n$ corresponding to the expansion coefficients α, β in eqn. (5). From these eigensolutions, the valence charge density is then calculated from

$$\rho(\mathbf{r}) = 2\sum_{n\mathbf{k}} f_{n\mathbf{k}} |\psi_{n\mathbf{k}}(\mathbf{r})|^2, \tag{9}$$

where $f_{n\mathbf{k}}$ is the occupancy of the state $\psi_{n\mathbf{k}}$.

In practice, the *k*-space summation was restricted to the irreducible part of the Brillouin zone. We tested convergence between 4 and 36 *k*-points, and estimate that our results are converged to within 5 mJ m^{-2}. Again, this is smaller than other sources of error.

4.2. *Twin boundary structure determination from first-principles*

To calculate the twin boundary energies, we first constructed a periodic array of twins from the relaxed EAM twin boundary structure at the bottom of figs. 3 and 4. We then used the above approach to calculate the energy of the appropriate 'unit cell' for the twin boundary array. The resulting twin boundary energy is given by

$$\Gamma = \frac{E_{\text{array}} - NE_{\text{hcp}}}{2A}, \tag{10}$$

where E_{array} is the energy of the unit cell that generates the array of twin boundaries, N is the number of atoms in this unit cell ($N = 12$ for these calculations), E_{hcp} is the energy per atom of a fully relaxed hcp structure, and A is the cross section of the unit cell taken parallel to the twin boundary. The factor of two arises because each unit cell will be intersected by two twin boundaries.

The fact that we are using a periodic array of twins, rather than isolated twins, will cause some inaccuracies in the values of the twin energies. The relaxations will be somewhat constrained by the small size of our system. To estimate the possible magnitude of error arising from the use of an array of twin boundaries rather than an isolated boundary, we performed a calculation of the energies of the twin boundaries using the EAM model of Zr with the periodic twin array. These results are also shown in table 3. As can be seen, this altered the twin boundary energies by less than 10%. More importantly, the ratio of the twin boundary energies (which, according to classical nucleation theory, controls the nucleation barrier) is almost unchanged.

Calculating accurate energies requires that the atomic positions be fully relaxed. In order to do this, we calculated the Hellman–Feynman forces using the well-converged

self-consistent band structures (Ho, Elsässer, Chan and Fähnle 1992) using corrections to the forces that accelerate the convergence of the forces (Chan, Bohnen and Ho 1993). Once the first-principles forces are calculated, we need to generate new positions. To do this, we calculated a force matrix using the EAM model. The force matrix is defined by

$$D_{i\alpha,j\beta} = \frac{\partial^2 U}{\partial x_{i\alpha} \partial x_{j\beta}}, \tag{11}$$

where $x_{i\alpha}$ is the displacement of atom i in the α direction. In the harmonic approximation, the forces are related to the displacements by

$$\mathbf{F} = -\mathbf{D} \cdot (\delta \mathbf{x}). \tag{12}$$

Knowing the forces, we can then estimate the displacements from the inverse of the force matrix. This gives us new positions, from which we can calculate a new set of forces. By iterating, we eventually achieve a set of positions for which the forces are negligible. The force matrix may also be corrected iteratively, according to the Broyden scheme (Broyden 1965).

§ 5. Twin boundary energies and discussion

The final twin boundary energies for Ti and Zr are shown in table 3, compared with the EAM model of § 2, and with other models for hcp metals. The structures are very similar to those found using our EAM model and displayed in figs. 3 and 4. The errors are calculated from our estimates of the possible error in relaxing the structures, amounting to approximately 7 meV per atom, and principally arise from the difficulty of calculating the total energy relative to the bulk hcp structure with the required precision.

The most important point is that the energies of the $\{10\bar{1}1\}$ twin boundary are significantly less than that of the $\{11\bar{2}2\}$ twin. Classical nucleation theory then would suggest that the $\{10\bar{1}1\}$ twin is more easily nucleated (Yoo and Lee 1991). At low temperatures (where entropic effects may be neglected) the reverse is observed: the $\{11\bar{2}2\}$ twin is significantly easier to form (Paton and Backofen 1970, Akhtar 1973). This indicates that the nucleation process is not well described by classical nucleation theory. The weakest assumption of classical nucleation theory is that the surface energy of a twin embryo is isotropic, equal to the twin boundary energy. Clearly, the surface energy will in fact be sensitive to the orientation, and will also entail defects such as twinning dislocations. A more general theory of twin nucleation is therefore required.

We note that the ratios of the twin boundary energies in Zr and Ti are, in fact, lower than that predicted from all empirical models. Our model for Zr is closer than the other models. However, although it predicts the structures fairly accurately, and produces a lower ratio of the twin boundary energies than other models, the EAM model does not produce particularly accurate twin boundary energies. The structures predicted by other models are essentially the same. The fact that this model similar to real Zr than the rest of the models of hcp materials suggests that this is a good empirical model for studying the deformation process in these metals.

Further work must concentrate on the formation and motion of twin boundaries. The relationship between the $\{11\bar{2}2\}$ twinning at low temperatures and $\{11\bar{2}2\}$ slip at high temperatures (Rosenbaum 1964) suggests that the observed change in behaviour is associated with a change in the dynamics of the associated dislocations. We are currently examining the structure of these dislocations, their dissociation into partial

dislocations, and their behaviour under stress. We believe that this will provide valuable insight into the nucleation process.

ACKNOWLEDGMENTS

This work was supported by the Director for Energy Research, Office of Basic Energy Sciences, and High Performance Computing and Communications initiative. In addition, we would like to acknowledge the Scalable Computing Laboratory at Ames Laboratory, the CCS at Oak Ridge National Laboratory, and the NERSC at Livermore National Laboratories for supplying computational resources. Ames Laboratory is operated for the US Department of Energy by Iowa State University under Contract No. W-7405-Eng-82. M.H.Y. acknowledges support by the Division of Materials Sciences, US Department of Energy, under Contract No. DE-AC05-84OR21400 with Martin Marietta Energy Systems.

REFERENCES

AKHTAR, A., 1973, *J. nucl. Mater.*, **47,** 79.
BACON, D. J., and SERRA, A., 1992, *Mater. Res. Soc. Symp. Proc.*, **238,** 73.
BREWER, L., 1975, Lawrence Berkeley Laboratory, Report No. 3720 (unpublished).
BROYDEN, C. G., 1965, *Math. Comp.*, **19,** 577.
CAMPBELL, G. H., FOILES, S. M., GUMBSCH, P., RÜHLE, M., and KING, W. E., 1993, *Phys. Rev. Lett.*, **70,** 449.
CHAN, C. T., BOHNEN, K. P., and HO, K. M., 1993, *Phys. Rev.* B, **47,** 4771.
CHEN, Y., FU, C. L., HO, K. M., and HARMON, B. N., 1985, *Phys. Rev.* B, **31,** 6775.
CLEMENTI, E., and ROETTI, C., 1974, *Atomic Data and Nuclear Data Tables*, Vol. 14, Nos. 3 and 4 (New York: Academic).
DAW, M. S., and BASKES, M. I., 1983, *Phys. Rev. Lett.*, **50,** 1285; 1984, *Phys. Rev.* B, **29,** 6443.
DAW, M. S., FOILES, S. M., and BASKES, M. I., 1993, *Mater. Sci. Reports*, **9,** 251.
ELSÄSSER, C., TAKEUCHI, N., HO, K. M., CHAN, C. T., BRAUN, P., and FÄHNLE, M., 1990, *J. Phys.* C, **2,** 4371.
FINNIS, M. W., and SINCLAIR, J. E., 1984, *Phil. Mag.* A, **50,** 45.
FISHER, E. S., and RENKEN, C. J., 1964, *Phys. Rev.* A, **135,** A482.
GOLDAK, J., LLOYD, L. T., and BARRETT, C. S., 1966, *Phys. Rev.*, **144,** 474.
HAMANN, D. R., SCHLÜTER, M., and CHIANG, C., 1979, *Phys. Rev. Lett.*, **43,** 1494.
HEDIN, L., and LUNDQVIST, B. I., 1971, *J. Phys.* C, **4,** 2064.
HEIMING, A., PETRY, W., TRANPENAU, J., ALBA, M., HERZIG, C., SCHOBER, H. R., and VOGL, G., 1988, *Phys. Rev.* B, **61,** 722.
HO, K. M., ELSÄSSER, C., CHAN, C. T., and FÄHNLE, M., 1992, *J. Phys.* C, **4,** 5189.
HO, K. M., FU, C. L., and HARMON, B. N., 1984, *Phys. Rev.* B, **29,** 1575.
IHM, J., ZUNGER, A., and COHEN, M. L., 1979, *J. Phys.* C, **12,** 4409.
JONES, R. O., and GUNNARSSON, O., 1991, *Rev. mod. Phys.*, **61,** 689.
KASUKABE, Y., YAMADA, Y., LIN, P. J., and BURSILL, L. A., 1993, *Phil. Mag. Lett.*, **67,** 361.
KERKER, G. P., 1980, *J. Phys. Chem.*, **13,** L189.
LEBENSOHN, R. A., and TOMÉ, C. N., 1993, *Phil. Mag.* A, **67,** 187.
LOUIE, S. G., HO, K. M., and COHEN, M. L., 1979, *Phys. Rev.* B, **19,** 1774.
MORRIS, J. R., YE, Y. Y., HO, K. M., CHAN, C. T., and YOO, M. H., 1994, *Phil. Mag. Lett.*, **69,** 189.
PATON, N. E., and BACKOFEN, W. A., 1970, *Metall. Trans.*, **1,** 2839.
POND, R. C., BACON, D. J., SERRA, A., and SUTTON, A. P., 1991, *Metall. Trans.* A, **22,** 1185.
ROSENBAUM, H. S., 1964, *Deformation Twinning*, Proceedings of the Metallurgical Society Conference, Gainesville, Florida, edited by R. E. Reed-Hill, J. P. Hirth, and H. C. Rogers (New York: Gordon and Breach), p. 43.
SERRA, A., and BACON, D. J., 1986, *Phil. Mag.* A, **54,** 793; 1991, *Ibid.*, **63,** 1001; 1993, *Mater. Sci. Forum*, **126–128,** 69.
SERRA, A., POND, R. C., and BACON, D. J., 1991, *Acta metall. Mater.*, **39,** 1469.
SINCLAIR, J. E., and FLETCHER, R., 1972, *J. Phys.* C, **7,** 864.

STASSIS, C., ZARESTKY, J., ARCH, D., MCMASTERS, O. D., and HARMON, B. N., 1978, *Phys. Rev.* B, **18,** 2632.
TAKEUCHI, N., CHAN, C. T., and HO, K. M., 1989, *Phys. Rev.* B, **40,** 1565.
YOO, M. H., 1981, *Metall. Trans.* A, **12,** 409.
YOO, M. H., FU, C. L., and LEE, J. K., 1991, *J. Phys.* III, **1,** 1065.
YOO, M. H., and LEE, J. K., 1991, *Phil. Mag.* A, **63,** 987.
ZHANG, B. L., WANG, C. Z., HO, K. M., TURNER, D. E., and YE, Y. Y., 1995, *Phys. Rev. Lett.*, **74,** 1375.